

## Interactions between cyclodextrins and fluorescent T-2 and HT-2 toxin derivatives: a physico-chemical study

Andrea Ventrella · Raffaella Verrone · Francesco Longobardi ·  
Angela Agostiano · Vincenzo Lippolis · Michelangelo Pascale ·  
Chris M. Maragos · Michael Appell · Lucia Catucci

Received: 3 October 2011 / Accepted: 16 February 2012 / Published online: 6 March 2012  
© Springer Science+Business Media B.V. 2012

**Abstract** T-2 and HT-2 toxins are mycotoxins produced by several *Fusarium* species that are commonly found in various cereal grains, including oats, barley, wheat and maize. Intake estimates indicate that the presence of these mycotoxins in the diet can be of concern for public health. In this work, the inclusion processes occurring between fluorescent anthracene-derivatives of T-2 and HT-2 toxins and different cyclodextrin (CD) molecules were investigated in aqueous solutions by means of UV–Vis absorption, fluorescence emission and dynamic light scattering. Binding constant values and chemico-physical parameters were calculated. It was found that  $\beta$ -CDs give stronger inclusion reactions with both T-2 and HT-2 derivatives, as stated by important emission intensity increments. Such interactions were found to be fundamentally enthalpy-driven. Among  $\beta$ -CDs, the effect of the methylation at hydroxyl groups was tested: as a result, the di-methyl form

of  $\beta$ -CD was found to induce the best fluorescence intensity enhancements.

**Keywords** T-2 toxin · HT-2 toxin · Cyclodextrin · Fluorescence · Inclusion complex

### Introduction

In the last few years, great attention has been addressed to mycotoxins due to their large diffusion in foodstuffs and feedstuffs worldwide and to their toxic effects on both animals and humans. Mycotoxins exhibit a variety of harmful biological effects, such as nephrotoxicity, hepatotoxicity, immunosuppression, carcinogenicity and in some cases they may be lethal, depending on many physical, chemical and biological factors [1–3]. As a consequence, mycotoxins represent not only a health threat, but an economical and social problem too, particularly in the underdeveloped countries.

T-2 and HT-2 toxins are type-A trichothecene mycotoxins produced mainly by several *Fusarium* species, mainly *Fusarium sporotrichioides*, *F. poae* and *F. langsethiae* [2, 4]. They are sesquiterpenoids, with an epoxidic ring on C12–C13 and a double bond on C9–C10.

T-2 and HT-2 toxins, as well as other trichothecenes, can be frequently found in various cereal crops (wheat, maize, barley, oat and rye) and processed grains (malt, beer and bread). The toxic effects of trichothecenes on animals have been extensively studied. On the contrary, little information is available about toxicity on humans. Nonetheless T-2 toxin is considered the most toxic trichothecene, since it is a potent inhibitor of DNA, RNA and protein synthesis and of mitochondrial functions. In addition it has been shown to have immunosuppressive and cytotoxic effects and to cause haematological damage and cell apoptosis [5–7]. HT-2 toxin is

---

A. Ventrella · R. Verrone · F. Longobardi · A. Agostiano ·  
L. Catucci (✉)  
Dipartimento di Chimica, Università degli Studi di Bari  
“Aldo Moro”, Via Orabona 4, 70126 Bari, Italy  
e-mail: catucci@chimica.uniba.it

A. Agostiano · L. Catucci  
IPCF-CNR, sez. Bari, Via Orabona 4, 70126 Bari, Italy

A. Agostiano  
INSTM, Via G. Giusti 9, 50121 Florence, Italy

V. Lippolis · M. Pascale  
Institute of Sciences of Food Production (ISPA), CNR-National  
Research Council of Italy, Via G. Amendola 122/O, 70126 Bari,  
Italy

C. M. Maragos · M. Appell  
Bacterial Foodborne Pathogens and Mycology Research Unit,  
USDA-ARS-NCAUR, Peoria, IL 61604, USA

an in vivo metabolite of T-2 toxin. Little information is available on the toxicity of HT-2 toxin alone, however studies seem to suggest that it has the same toxic effects of T-2 toxin and similar potency. Even the Joint FAO/WHO Expert Committee on Food Additives (JECFA) indicated that the toxic effects of T-2 toxin can not be distinguished from those of HT-2 toxin and that the two trichothecenes can act simultaneously.

The only authoritative safety indication has been given by JECFA. They developed a Provisional tolerable daily intake (PTDI) of 60 ng/kg bw for the two toxins alone or combined [8]. More detailed regulatory limits are expected.

Different analytical methods are available for sensitive determination of type-A trichothecenes, such as immunoassays, gas chromatography (GC) with electron capture (ECD), mass spectrometry (MS) or flame ionization (FID) detectors, and high pressure liquid chromatography (HPLC) coupled with atmospheric pressure chemical ionization MS [9–11]. The greatest limitation is the lack of appropriate chromophores in type-A trichothecenes, that makes HPLC with UV or fluorescence detectors (FLD) poorly applicable. On the other hand, methods using HPLC with FLD for determination of T-2 and HT-2 toxins have been recently developed, based on a derivatization process, in which a chromophore is linked to the toxin structure. Up to now, different derivatizing reagents have been proposed for fluorescent labelling of some type-A trichothecenes. These include coumarin-3-carbonyl chloride (not commercially available), 1-anthroylnitrile (1-AN), 1-naphthoyl chloride (1-NC), 2-naphthoyl chloride (2-NC) and pyrene-1-carbonyl-cyanide (PCC) [12–15]. 1-AN has been applied for the simultaneous determination of T-2 and HT-2 toxins in wheat, maize, and barley by HPLC-FLD after immunoaffinity column clean-up. The method allowed the determination of anthracene-derivatives of T-2 and HT-2 toxins (Fig. 1) at levels of 5 and 3  $\mu\text{g kg}^{-1}$  (LOD, limit of detection), respectively, with good accuracy and precision [13].

Efforts to increase the emission intensity of T-2 and HT-2 fluorescent derivatives can be considered as a logical consequence of the need to find more sensitive, accurate and reliable analytical methods for their detection to be used for mycotoxin risk assessment studies.

It is known that the emission of many fluorophores is sensitive to the local environment [16, 17]. Certain cyclodextrins (CDs) have the ability to form inclusion complexes, changing the physico-chemical properties of the guest molecule, which is why CDs are a promising tool to aid detection [18, 19]. In particular, it has been demonstrated that several mycotoxin molecules show an enhancement of fluorescence upon inclusion with CDs under certain conditions [16]. Such effect can be particularly useful to increase the sensitivity of guest luminescence-based detection methods.

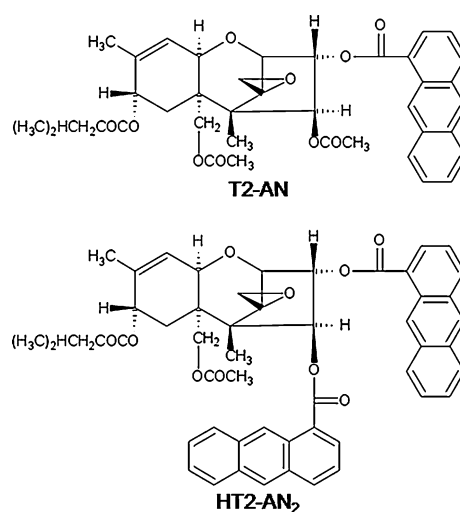


**Fig. 1** Chemical structures of the anthracene-derivatives of T-2 (T2-AN) and HT2 (HT2-AN<sub>2</sub>)

In this work, the interactions occurring between the anthracene (AN) derivatives of T-2 and HT-2 toxins, indicated as T2-AN and HT2-AN<sub>2</sub>, and CDs were investigated by means of optical techniques, i.e. UV–Vis absorption, fluorescence emission and Dynamic light scattering (DLS) spectroscopies, in order to evaluate which CDs could be considered more useful and suitable tools for the enhancement of T2-AN and HT2-AN<sub>2</sub> emission signals. The binding constants and complex stoichiometries of inclusion complexes, as well as the thermodynamic parameters relevant to complexation processes were calculated. Molecular models of the guest–host inclusion complexes supported the experimentally derived complexation processes. This research demonstrated the use of inclusion complexes to improve detection of natural contaminants.

## Experimental

### Chemicals

$\alpha$ -CD,  $\beta$ -CD, heptakis-2,6-di-*O*-methyl- $\beta$ -CD (DIMEB), heptakis-2,3,6-tri-*O*-methyl- $\beta$ -CD (TRIMEB),  $\gamma$ -CD were purchased from Sigma-Aldrich and used without further purification. Acetonitrile (ACN, HPLC grade) and toluene (for organic residue analysis) were purchased from Mallinckrodt Baker. Ultrapure water was produced with a Millipore Milli-Q system. T-2 toxin, HT-2 toxin and 4-dimethylaminopyridine (DMAP) were purchased from Sigma-Aldrich, while 1-AN was from Wako.

### Synthesis and purification of anthracene-derivatives of T-2 and HT-2 toxins

The syntheses of the anthracene-derivatives of T-2 (T2-AN) and HT-2 toxins (HT2-AN<sub>2</sub>) have been separately performed

according to the procedure previously reported in the literature [13], by an acylation with 4-dimethylaminopyridine (DMAP) as reaction catalyst. The purification of the derivatives was performed by HPLC, using a Varian ProStar system equipped with Waters Symmetry Prep C18 column ( $150 \times 7.8 \text{ mm}^2$ ,  $7 \mu\text{m}$ ) and fluorescence detector ( $\lambda_{\text{exc}} = 381 \text{ nm}$ ;  $\lambda_{\text{em}} = 470 \text{ nm}$ ). The mobile phase, at a flow rate of  $3.5 \text{ mL min}^{-1}$ , was ACN/water 70:30 (v/v) for T2-AN, and ACN/water 88:12 (v/v) for HT2-AN<sub>2</sub>. Aliquots of the reaction mixtures were injected. Fractions eluting between 16.3 and 20.9 min in the purification of T2-AN, and between 13.8 and 16.8 min in the purification of HT2-AN<sub>2</sub> were collected from the column. The fractions were pooled and the solvent was removed by a combination of vacuum evaporation and lyophilization.

#### Preparation of toxin and toxin/CD aqueous solutions

T2-AN and HT2-AN<sub>2</sub> stock solutions ( $5 \times 10^{-3} \text{ M}$ , determined by gravimetric analysis) in ACN were stored in the dark at  $4 \text{ }^\circ\text{C}$ . Aqueous stock solutions of CDs ( $3.63 \times 10^{-3} \text{ M}$ ) were prepared in ultrapure water at pH 7.5.

In order to prepare toxin and toxin/CD aqueous solutions, the appropriate amount of the stock solution of the toxin was completely dried under N<sub>2</sub> stream. The toxin solid residue was then added with water and CD-water solution and stirred on a vortex for more than a minute to favour dissolution. For routine spectroscopic characterization, the toxin solid residue was dissolved in ACN/water 70:30 (v/v).

The final derivative concentration realized in the investigated solutions was  $1.5 \times 10^{-7} \text{ M}$ . While the CD concentration varied as reported in the “Results and discussion” section.

#### Absorption, steady-state fluorescence and DLS measurements

UV–Visible absorption spectra were recorded using a Varian Cary/3 spectrophotometer. Fluorescence measurements were realized using a Varian Cary Eclipse

spectrofluorometer. Both measurements were performed using a 1 cm path length quartz cell.

DLS experiments were performed by means of a Horiba LB-550 Nanoparticle Size Analyzer.

#### Molecular modeling

Molecular mechanics geometry optimization calculations were carried out on cyclodextrin-trichothecene derivative complexes using the Merck Molecular Force Field (MMFFaq) and the aqueous Solvation Model 5.4 (SM5.4) as implemented in Spartan’10 (<http://www.wavefun.com/>). The geometry optimization calculations were carried out with a gradient of  $3 \times 10^{-4}$  Hartree/Bohr. Final geometries are displayed using Hyperchem software v8.0.9 ([www.hyperchem.com](http://www.hyperchem.com)).

## Results and discussion

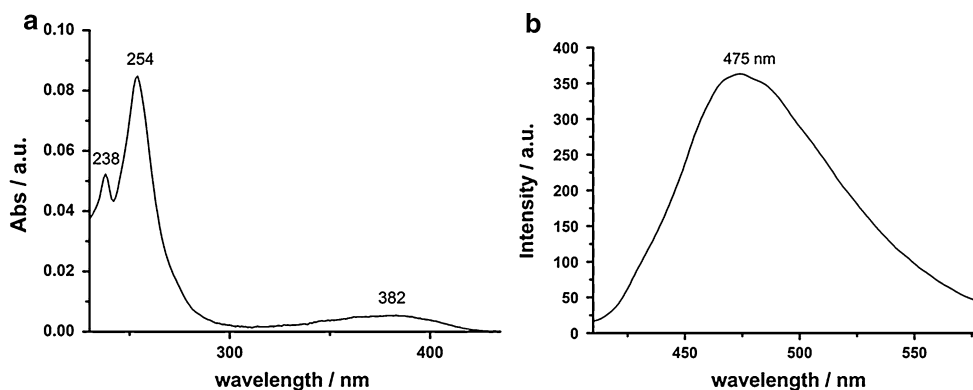
The T-2 toxin derivative was characterized by spectroscopic analyses. Due to the very low solubility of this toxin derivative in water, the routine characterization was performed on a water-ACN mixture. In Fig. 2a, the absorption spectrum of  $1.4 \times 10^{-5} \text{ M}$  T2-AN in ACN:water 70:30 (v/v) is reported; this solvent mixture is typically used in HPLC purification of the derivative.

The derivative exhibits three main absorption maxima in the range 200–550 nm at 238, 254, and 382 nm, that correspond to  $\pi \rightarrow \pi^*$  electronic transitions in the anthracene moiety.

The fluorescence emission spectrum (Fig. 2b) shows a peak at 475 nm. Since many CDs can absorb at wavelengths below 250 nm, all fluorescence spectra and data reported in this work were obtained by exciting at 382 nm.

The effect of the presence of the three un-modified CDs,  $\alpha$ -  $\beta$ - and  $\gamma$ -CD, on T2-AN spectroscopic properties was evaluated in water solutions. For the screening, the toxin derivative concentration was kept at  $1.5 \times 10^{-7} \text{ M}$  in all the aqueous solutions used and the concentration of CDs in

**Fig. 2** **a** Absorption spectrum of an ACN:water solution of T2-AN  $1.4 \times 10^{-5} \text{ M}$ . **b** Fluorescence spectrum of an ACN:water solution of T2-AN  $1.4 \times 10^{-5} \text{ M}$



the prepared solutions was  $2.5 \times 10^{-3}$  M. As can be observed in Fig. 3, the presence of CDs induced a significant enhancement of fluorescence intensity.

It is evident that  $\beta$ -CD caused the greatest fluorescence increase. This particular behaviour suggests that  $\beta$ -CD cavity is more suitable to form inclusion complexes with T2-AN, enhancing its emission intensity. In particular, it can be supposed that the interaction mainly involves the anthracene moiety of the toxin derivative, since it represents the fluorophore group of this molecule. The  $\gamma$ -CD produced a less intense fluorescence enhancement, i.e. less rigidity of the fluorophore inside the CD cavity, probably due to its greater dimensions, allowing only weaker interactions with the toxin derivative. These considerations are in accordance with data in the literature [20].

The presence of  $\alpha$ -CD caused only a slight fluorescence enhancement, probably due to its too small cavity dimensions, that do not allow T2-AN to be well included, in accordance with previous studies showing that anthracene can form a very weak association with  $\alpha$ -CD [21]. Therefore, non-inclusion interactions are more likely to occur in this case. Because of these observations, more attention was focused on  $\beta$ -CD and its derivatives: DIMEB and TRIMEB. The structural consequences of substituting CD hydroxyl with methyl groups can be observed in the changes of the CD size: according to Sen et al. [22] and to Gaitano and Brown [23], the height of an unsubstituted  $\beta$ -CD is 7.90 Å, while the height of a DIMEB (or TRIMEB) cavity is slightly longer (10.9 Å), because of the extra methyl groups. Such structural changes, together with the steric effect of the methyl substituents, can affect the CD tendency to form inclusion complexes.

Aqueous solutions of these differently methylated  $\beta$ -CDs were tested by keeping the T2-AN concentration

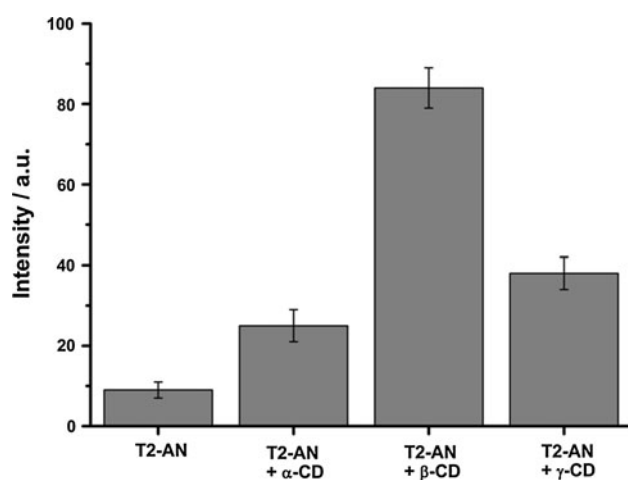


**Fig. 3** Fluorescence intensities at peak wavelength for  $1.5 \times 10^{-7}$  M T2-AN solutions in the absence and in the presence of  $2.5 \times 10^{-3}$  M natural CDs. Reported data represent mean values  $\pm$  standard deviations obtained from three replicates

constant, and varying the CD type and concentration. Fluorescence measurements on all these solutions evidenced that all the studied  $\beta$ -CDs were able to enhance T2-AN emission intensities, and that such enhancements depended on the CD concentration.

In Fig. 4 the fluorescence intensities of T2-AN/ $\beta$ -CDs solutions, recorded at the maximum emission wavelength, are observable. It can be seen that all three  $\beta$ -CDs induced a fluorescence enhancement and that high emission (about 200 a.u.) was recorded in the presence of  $1.6 \times 10^{-3}$  M DIMEB.  $\beta$ -CD was found to induce such fluorescence enhancement only at much higher concentrations (about  $8 \times 10^{-3}$  M) while TRIMEB promoted lower toxin fluorescence enhancements at all concentrations studied. Probably, in the case of DIMEB the two methyl groups could confer rigidity to the host molecule, such that the loss of rotational freedom can be optimal to produce higher fluorescence enhancements.

The binding constants of the inclusion complexes and their stoichiometries in the temperature range 25–40 °C were calculated, by applying a modified Benesi-Hildebrand [24] equation (Eq. 1), and thermodynamic parameters, by means of the Van't Hoff equation (Eq. 2).

$$F_0/(F - F_0) = 1/A + 1/(AK[CD]^n) \quad (1)$$

$$\ln K = -\Delta H^\circ/(RT) + \Delta S^\circ/R \quad (2)$$

In Eq. 1, for a given temperature ( $T$ ),  $K$  is the binding constant,  $F_0$  is the initial fluorescence intensity of free toxin,  $F$  is the maximum fluorescence intensity of the CD-toxin inclusion complexes at the considered CD concentration,  $A$  is a constant, and  $n$  is the number of binding sites. In Eq. 2,  $\Delta H^\circ$  and  $\Delta S^\circ$  are the variations of

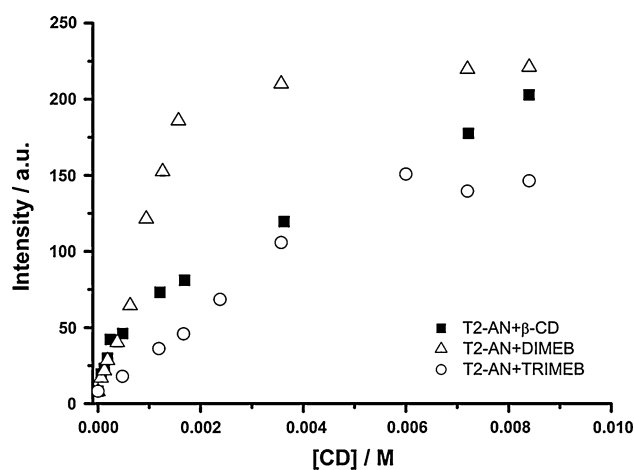


**Fig. 4** T2-AN aqueous solution fluorescence intensities at peak wavelength in the presence of natural and methylated  $\beta$ -CDs. Solutions with T2-AN and  $\beta$ -CDs, DIMEB or TRIMEB are indicated in the graph by *full squares*, *empty triangles* and *empty circles*, respectively

**Table 1** T2-AN/CD binding constants at 25 °C, complex stoichiometry and thermodynamic parameters; data represent mean values  $\pm$  standard deviations obtained from three replicates

CD	Complex stoichiometry	$K_{\text{binding, 25 } ^\circ\text{C}}$	$\Delta H^\circ$ (kJ/mol)	$\Delta S^\circ$ (J/K mol)	$\Delta G^\circ$ (kJ/mol)
$\beta$ -CD	1:1	$963 \pm 36 \text{ M}^{-1}$	$-14 \pm 2$	$18 \pm 7$	$-19 \pm 4$
	2:1	$76,800 \pm 120 \text{ M}^{-2}$	$22 \pm 3$	$150 \pm 10$	$-23 \pm 6$
DIMEB	1:1	$716 \pm 19 \text{ M}^{-1}$	$-69 \pm 7$	$-180 \pm 20$	$-15 \pm 5$
TRIMEB	1:1	$19 \pm 5 \text{ M}^{-1}$	$-91 \pm 1$	$-271 \pm 20$	$-10 \pm 4$

enthalpy and entropy associated with the inclusion process, respectively, while  $R$  is the universal gas constant.

Values of the binding constants of the complexes formed by inclusion of the anthracene moiety of T2-AN into the CD cavities and the relevant stoichiometries at 25 °C are reported in Table 1.

As it can be seen in the investigated CD concentration ranges, both DIMEB and TRIMEB induced only the formation of 1:1 inclusion complexes, since the best linear fittings were achieved when a 1:1 stoichiometry ( $n$  equal to 1) was considered in Eq. 1.  $\beta$ -CD showed a different behaviour: in particular, it was evidenced the formation of 1:1 inclusion complexes up to the concentration of  $2.4 \times 10^{-3} \text{ M}$ ; on the other hand, at higher CD concentrations, only if a 2:1 stoichiometry is considered it is possible to fit the experimental data by the Benesi-Hildebrand equation. This observation is in accordance with recent studies that demonstrate that  $\beta$ -CDs show tendency to aggregation in water and that its critical aggregation concentration (c.a.c.) is in the range  $2 \times 10^{-3}$ – $3 \times 10^{-3} \text{ M}$  [25, 26]. The  $\beta$ -CD aggregates are reported to be micrometric, planar and consistent with head-to-head or tail-to-tail configurations. Therefore, when the  $\beta$ -CD is in its monomeric form, it allows the formation of 1:1 inclusion complexes, while when it is aggregated, its planar aggregates are involved in the formation of 2:1 complexes, that could be both inclusion and non-inclusion complexes, as reported by Loftsson et al. [27]. DIMEB and TRIMEB differ from natural  $\beta$ -CD for bearing methyl groups, and molecular dynamics calculations reported by Bikadi et al. [28] demonstrated that the methylated  $\beta$ -CDs possess low tendency to aggregate. Hence, in this work for these methylated CDs only the formation of 1:1 inclusion complexes was observed.

The thermodynamic data, reported in Table 1, suggest that for all the 1:1 inclusion complexes, the “driving force” in the complexation process is the enthalpy variation,  $\Delta H^\circ$ , attributable to the formation of hydrogen bonds or to electrostatic interactions, between T2-AN and the  $\beta$ -CDs. Only in the case of  $\beta$ -CD 2:1 complex the “driving force” is represented by the entropy variation,  $\Delta S^\circ$ . In this case, in fact, the interaction existing between T2-AN and the  $\beta$ -CD brought about the break of CD planar aggregates, as confirmed by the DLS analyses (Fig. 5), with a resulting entropy increase.

From the figure, indeed, it is evident that  $\beta$ -CD gave rise to large aggregates, with diameters equal to 1100 nm, at concentration values higher than its c.a.c.

These measurements are in accordance with the data reported by Bonini et al. [25], who demonstrated that above 3 mM concentration in water,  $\beta$ -CD is able to form aggregates ranging from about the hundred nm to micrometer in size. The relevant amounts and ratios depend upon the  $\beta$ -CD concentration itself (the formation of such self-assembled aggregates and their interaction with water are responsible for the particularly low solubility of  $\beta$ -CD in water, when compared to  $\alpha$ - and  $\gamma$ -CD); similar aggregates are not reported to form at concentrations lower than 3 mM. Addition of the guest T2-AN caused a breaking of these aggregates, and the average detected diameter resulted to be about 2.6 nm, whereas at  $\beta$ -CD concentration lower than c.a.c., it was not possible to detect any signal over the lower limit of detection of the instrument.

In Table 1 it can be observed that although a positive  $\Delta S^\circ$  contribution was calculated also for the formation of  $\beta$ -CD/T2-AN 1:1 complexes, in the cases of the 1:1 complexes involving DIMEB and TRIMEB negative  $\Delta S^\circ$

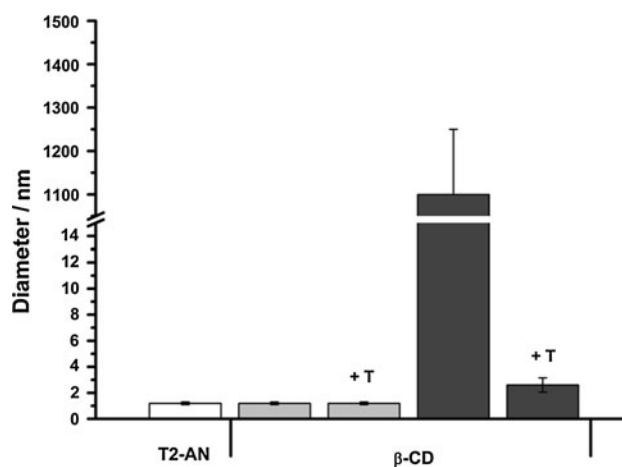


**Fig. 5** DLS measured diameters for T2-AN,  $\beta$ -CD and T2-AN/ $\beta$ -CD solutions. The symbol +T indicate the addition of T2-AN to  $\beta$ -CD solutions. Concentration of T2-AN was  $1.5 \times 10^{-5} \text{ M}$ , while CD concentrations used were 0.0005 M (light grey bars) and 0.007 M (dark grey bars). Reported data represent mean values  $\pm$  standard deviations obtained from three replicates

contributions were obtained. This difference could be due to the effects of the number of methyl substituents on  $\beta$ -CD (that increases in the direction  $\beta$ -CD > DIMEB > TRIMEB). Indeed, it is reported that methyl derivatives of CDs can host a lower number of water molecules inside their cavities, and this can affect the energy parameters involved in the inclusion process. In particular the cavity of a  $\beta$ -CD is reported to host nine water molecules [29, 30], while DIMEB can include one water molecule [31]. The dynamics of CD-water or water–water hydrogen bond breaking/formation are really important to understand the general energy balance involved in the inclusion process of CDs, and it is known that the water molecules inside the cavity of the CDs are more energetic than the ones in the bulk phase [29].

In the case reported in this paper it can be seen that the higher the number of methyl substituents, the more negative the entropic contribution: indeed, the  $\beta$ -CD can release a higher number of water molecules than its methylated forms DIMEB and TRIMEB and then include the T2-AN molecule; each water molecule that goes from inside the cavity towards the bulk phase can give a positive contribution to the entropy and if the sum of these water contributions overtakes the negative contribution due to the formation of the ordered complex molecule CD/T2-AN (reduced conformational freedom of host and guest), the general balance of  $\Delta S^\circ$  can be positive, as observed for  $\beta$ -CD.

Analogous results were obtained for HT2-AN<sub>2</sub> that showed absorption and emission spectra similar to T2-AN (spectra not shown), due to the presence of the same chromophore groups. In particular, high values of the binding constants were obtained in the presence of the different  $\beta$ -CDs. As for T2 derivative, it was found that the addition of DIMEB to HT2-AN<sub>2</sub>  $1.5 \times 10^{-7}$  M water solution gave rise to the most significant fluorescence enhancement with respect to the other CDs under investigation. Fluorescence measures were performed at different temperatures (20–35 °C) and data were treated by means of Eq. 1 and subsequently by Eq. 2. At 25 °C the best linear fitting was obtained by considering a 2:1 CD:guest stoichiometry, with a calculated binding constant equal to  $17,000 \pm 4,000 \text{ M}^{-2}$ . The complex stoichiometry is consistent with the presence on each derivative molecule of two anthracene moieties, both able to be included in a CD cavity. Therefore, it can be said that HT2-AN<sub>2</sub> molecule has two binding sites (the two anthracene moieties) and both of them are included in the cavities of two DIMEB molecules, giving rise to a 2:1 complex. This would account for the high value of the binding constant and for the values of the thermodynamic parameters that were subsequently calculated ( $\Delta H^\circ$  equal to  $-85 \text{ kJ/mol}$ ,  $\Delta S^\circ$  equal to  $-200 \text{ J/mol K}$  and  $\Delta G_{25^\circ\text{C}}$  equal to  $-25 \text{ kJ/mol}$  calculated by means of Van't Hoff equation), and in

particular for the high absolute  $\Delta H^\circ$  value, that even in this case, makes the complexation process enthalpy-driven.

In order to support the experimental data and the thermodynamic treatment, MMFF calculations were employed to obtain models of the trichothecene derivatives: CD complex formation; in particular, the energies associated with the complex formation (Table 2) and the structures of the complexes (Fig. 6) were obtained and here shown considering  $\beta$ -CD and DIMEB. As it can be seen, in all models, the anthracene moiety was accommodated within the  $\beta$ -CD and DIMEB cavities. In the complex of  $\beta$ -CD:T2-AN (2:1), one  $\beta$ -CD formed a complex with the anthracene moiety and a second  $\beta$ -CD interacted with the isovalerate moiety of T2-toxin.

The energy associated with the complex formation between trichothecene derivatives and CD,  $\Delta E_{\text{complexation}}$ , was determined through the following relationship:

$$E_{\text{Complexation}} = E_{\text{Complex}} - (E_{\text{CD}} + E_{\text{T2/HT2}}) \quad (3)$$

where  $E_{\text{complex}}$  is the energy of the trichothecene-CD complex,  $E_{\text{CD}}$  is the energy of the geometry optimized free CD host, and  $E_{\text{T2/HT2}}$  is the energy of the optimized free T2 or HT2 toxin derivative guest [32]. The magnitude of  $\Delta E_{\text{complexation}}$  indicates the driving force toward complex formation. The negative values for the  $\Delta E_{\text{complexation}}$  by the MMFF calculations with implicit aqueous solvation suggested the formation of the inclusion complexes is energetically favoured under aqueous conditions [33].

## Conclusions

The purpose of this work was to evaluate which kind of CD could produce stronger interactions with T2-AN or HT2-AN<sub>2</sub> toxin derivatives, thus giving rise to more important and evident changes in the chemico-physical properties of the guest molecules and in particular in the emission intensity enhancements, since fluorescence emission is used to detect such toxins.

Investigations on the interaction between toxin derivatives and CDs showed that complexes can be formed with  $\beta$ -CDs in water solutions by the inclusion of their anthracene moieties. This was evidenced by increments in the emission intensities of the toxin derivatives in the presence of CDs. In

**Table 2** Calculated complexation energies of the complexes formed by trichothecene derivatives with  $\beta$ -CD and DIMEB

Structure	Complex	$\Delta E_{\text{complexation}}$ (kcal mol <sup>-1</sup> )
a	$\beta$ -CD:T2-AN (1:1)	-20.65
b	DIMEB:T2-AN (1:1)	-12.77
c	$\beta$ -CD:T2-AN (2:1)	-46.76
d	DIMEB:HT2-AN <sub>2</sub> (2:1)	-52.75

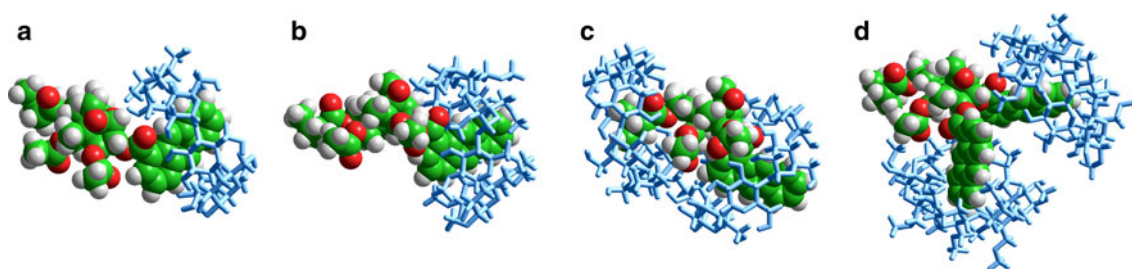


**Fig. 6** Geometry optimized structures of CD-trichothecene derivative complexes, **a**  $\beta$ -CD:T2-AN 1:1, **b** DIMEB:T2-AN 1:1, **c**  $\beta$ -CD:T2-AN 2:1, **d** DIMEB:HT2-AN<sub>2</sub> 2:1

particular, natural  $\beta$ -CD, DIMEB and TRIMEB formed 1:1 inclusion complexes with T2-AN, even if at concentration values higher than the c.a.c.,  $\beta$ -CD was found to form 2:1 complexes with this toxin derivative. This latter behaviour was consistent with data in the literature asserting that  $\beta$ -CD has tendency to aggregate in water solutions when its concentration exceeds the c.a.c. value ( $>2 \times 10^{-3}$  M) and that such aggregates can be broken in the presence of suitable guest molecules. The rupture of the  $\beta$ -CD planar micrometric aggregates by T2-AN was here evidenced by DLS measurements. On the contrary, DIMEB and TRIMEB, due to the presence of methyl groups, showed lower tendencies to aggregate, in accordance with the literature. In particular DIMEB gave rise to the highest fluorescence intensity measurements in the presence of T2-AN, as well as for HT2-AN<sub>2</sub> (whose complexation stoichiometry was 2:1, due to the presence of two anthracene moieties). The inclusion complex formation for  $\beta$ -CD and DIMEB with T2-AN and HT2-AN<sub>2</sub> was supported by molecular mechanics calculations. All these observations were confirmed by calculating the thermodynamic parameters, which showed that the complex formations involving non aggregated  $\beta$ -CDs were enthalpy-driven, while the reactions between  $\beta$ -CD aggregates and toxin derivatives were found to be entropy-driven.

**Acknowledgment** This study was supported by PRIN 2008 “Architetture ibride multifunzionali basate su biomolecole per applicazioni nel campo della sensoristica, della conversione di energia e del biomedicale”.

**Disclaimer** The mention of trade names or commercial products in this publication is solely for the purpose of providing specific information and does not imply recommendation or endorsement by the U.S. Department of Agriculture. The USDA is an equal opportunity provider and employer.

## References

- D’Mello, J.P.F., MacDonald, A.M.C.: Mycotoxins. *Anim. Feed Sci. Technol.* **69**, 155–166 (1997)
- Miller, J.D.: Fungi and mycotoxins in grains: implications for stored product research. *J. Stor. Prod. Res.* **31**, 1–16 (1995)
- Yiannikouris, A., Jouany, J.P.: Mycotoxins in feed and their fate in animals: a review. *Anim. Res.* **51**, 81–99 (2002)
- Edwards, S.G., Barrier-Guillot, B., Clasen, P.E., Hietaniemi, V., Pettersson, H.: Emerging issues of HT-2 and T-2 toxins in European cereal production. *World Mycotoxin J.* **2**, 173–179 (2009)
- Ishigami, N., Shinozuka, J., Katayama, K., Uekama, K., Nakayama, H., Doi, K.: Apoptosis in the developing mouse embryos from T-2 toxin-inoculated dams. *Histol. Histopathol.* **14**, 729–733 (1999)
- Islam, Z., Nagase, M., Ota, A., Ueda, S., Yoshizawa, T., Sakato, N.: Structure-function relationship of T-2 toxin and its metabolites in inducing thymic apoptosis in vivo in mice. *Biosci. Biotechnol. Biochem.* **62**, 1492–1497 (1998)
- Shinozuka, J., Suzuki, M., Noguchi, N., Sugimoto, T., Uetsuka, K., Nakayama, H., Doi, K.: T-2 toxin-induced apoptosis in hematopoietic tissues of mice. *Toxicol. Pathol.* **26**, 672–681 (1998)
- Canady, R.A., Coker, R.D., Egan, S.K., Krska, R., Olsen, M., Resnik, S., Schlatter, J.: T-2 and HT-2 toxins. In: safety evaluation of certain mycotoxins in food, WHO food additives series 47, FAO food and nutrition paper 74, pp. 557–638. Joint FAO/WHO Expert Committee on Food Additives (JECFA), WHO, Geneva (2001)
- Koch, P.: State of the art of trichothecene analysis. *Toxicol. Lett.* **153**, 109–112 (2004)
- Krska, R., Baumgartner, S., Josephs, R.: The state-of-the-art in the analysis of type-A and -B trichothecene mycotoxins in cereals. *Fresenius J. Anal. Chem.* **371**, 285–299 (2001)
- Rasmussen, P.H., Ghorbani, F., Berg, T.: Deoxynivalenol and other *Fusarium* toxins in wheat and rye flours on the Danish market. *Food Addit. Contam.* **20**, 396–404 (2003)
- Pascale, M., Haidukowski, M., Visconti, A.: Determination of T-2 toxin in cereal grains by liquid chromatography with fluorescence detection after immunoaffinity column clean-up and derivatization with 1-anthrolynitrite. *J. Chromatogr. A* **989**, 257–264 (2003)
- Visconti, A., Lattanzio, V.M.T., Pascale, M., Haidukowski, M.: Analysis of T-2 and HT-2 toxins in cereal grains by immunoaffinity clean-up and liquid chromatography with fluorescence detection. *J. Chromatogr. A* **1075**, 151–158 (2005)
- Maragos, C.M.: Measurement of T-2 and HT-2 toxins in eggs by high-performance liquid chromatography with fluorescence detection. *J. Food Prot.* **69**, 2773–2776 (2006)
- Lippolis, V., Pascale, M., Maragos, C.M., Visconti, A.: Improvement of detection sensitivity of T-2 and HT-2 toxins using different fluorescent labelling reagents by high-performance liquid chromatography. *Talanta* **74**, 1476–1483 (2008)
- Maragos, C.M., Appell, M., Lippolis, V., Visconti, A., Catucci, L., Pascale, M.: Use of cyclodextrins as modifiers of fluorescence in the detection of mycotoxins. *Food Addit. Contam.* **25**, 164–171 (2008)

17. Vázquez, M.L., Cepeda, A., Prognon, P., Mahuzier, G., Blaus, J.: Cyclodextrins as modifiers of the luminescence characteristics of aflatoxins. *Anal. Chim. Acta* **255**, 343–350 (1991)
18. Verrone, R., Catucci, L., Cosma, P., Fini, P., Agostiano, A., Lippolis, V., Pascale, M.: Effect of beta-cyclodextrin on spectroscopic properties of ochratoxin A in aqueous solution. *J. Incl. Phenom. Macrocycl. Chem.* **57**, 475–479 (2007)
19. Fini, P., Castagnolo, M., Catucci, L., Cosma, P., Agostiano, A.: The effects of increasing NaCl concentration on the stability of inclusion complexes in aqueous solution. *J. Therm. Anal. Calorim.* **73**, 653–659 (2003)
20. Li, C., Mu, J., Zhang, Y.: Study on effects of cyclodextrins on the photolysis of dissolved anthracene by fluorometry. *Luminescence* **20**, 261–265 (2005)
21. Blyshak, L.A., Warner, I.M., Patonay, G.: Evidence for non-inclusion association between  $\alpha$ -cyclodextrin and polynuclear aromatic hydrocarbons. *Anal. Chim. Acta* **232**, 239–243 (1990)
22. Sen, P., Roy, D., Mondal, S.K., Sahu, K., Ghosh, S., Bhattacharyya, K.: Fluorescence anisotropy decay and solvation dynamics in a nanocavity: coumarin 153 in methyl  $\beta$ -cyclodextrins. *J. Phys. Chem. A* **109**, 9716–9722 (2005)
23. Gaitano, G.G., Brown, W.: Inclusion complexes between cyclodextrins and triblock copolymers in aqueous solution: a dynamic and static light-scattering study. *J. Phys. Chem. B.* **101**, 710–719 (1997)
24. Indirapriyadharshini, V.K., Karunanithi, P., Ramamurthy, P.: Inclusion of resorcinol-based acridinedione dyes in cyclodextrins: fluorescence enhancement. *Langmuir* **17**, 4056–4060 (2001)
25. Bonini, M., Rossi, S., Karlsson, G., Almgren, M., Lo Nostro, P., Baglioni, P.: Self-assembly of  $\beta$ -cyclodextrin in water. Part I: cryo-TEM and dynamic and static light scattering. *Langmuir* **22**, 1478–1484 (2006)
26. Rossi, S., Bonini, M., Lo Nostro, P., Baglioni, P.: Self-assembly of  $\alpha$ -cyclodextrin in water. 2. Electron spin resonance. *Langmuir* **23**, 10959–10967 (2007)
27. Loftsson, T., Másson, M., Brewster, M.E.: Self-association of cyclodextrins and cyclodextrin complexes. *J. Pharm. Sci.* **93**, 1091–1099 (2004)
28. Bikadi, Z., Kurdi, R., Balogh, S., Szeman, J., Hazai, E.: Aggregation of cyclodextrins as an important factor to determine their complexation behavior. *Chem. Biodivers.* **3**, 1266–1278 (2006)
29. Buschmann, H.J., Dong, H., Schollmeyer, E.: Complexation of aliphatic alcohols by  $\alpha$ - and  $\beta$ -cyclodextrins and their partial methylated derivatives in aqueous solution. *J. Therm. Anal. Calorim.* **61**, 23–28 (2000)
30. Saenger, W., Noltemeyer, M., Manor, P.C., Hingerty, B., Klar, B.: “Induced-fit”-type complex formation of the model enzyme  $\alpha$ -cyclodextrin. *Bioorg. Chem.* **5**, 187–195 (1976)
31. Aree, T., Saenger, W., Leibnitz, P., Hoier, H.: Crystal structure of heptakis(2,6-di-*O*-methyl)- $\beta$ -cyclodextrin dihydrate: a water molecule in an apolar cavity. *Carbohydr. Res.* **315**, 199–205 (1999)
32. Barbiric, D.J., de Rossi, R.H., Castro, E.A.: Inclusion complexes of 1:2 stoichiometry between azobenzenes and cyclodextrins: a molecular mechanics study. *J. Mol. Struct. (Theochem)* **537**, 235–243 (2001)
33. Rodrigues, S.G., Chaves, I.S., de Melo, N.F.S., de Jesus, M.B., Fraceto, L.F., de Fernandes, S.A., Paula, E., de Freitas, M.P., Pinto, L.M.A.: Computational analysis and physico-chemical characterization of an inclusion compound between praziquantel and methyl  $\beta$ -cyclodextrin for use as an alternative in the treatment of schistosomiasis. *J. Incl. Phenom. Macrocycl. Chem.* **70**, 19–28 (2011)